the spin of μ^-, a particle, must point in the direction opposite to its momentum. This seems to be consistent with the present observation. It must be noticed, however, that the $\mu-e$ decay itself is insensitive to which of μ^+ and μ^- is the particle or antiparticle.

Another advantage of the two-component theory is that it enables us to predict the degree of longitudinal polarization of decay electrons if only the $\cos\theta$ dependence of the spectrum (2.19) is known. This was mentioned in reference 6 and also in the paragraph (f) of Sec. 2. It is thus inferred from experimental data that, averaged over the angle θ, at least 88% of the electrons (or positrons) from the muon decay are polarized parallel (antiparallel) to their motion if the two-component theory is valid. The polarization of the muon spin at the moment of decay can also be measured by looking at the electron polarization.[6]

In our discussion, we have neglected completely the effect of the electron mass on the decay spectrum. Comparison of (2.5) with the exact formula[25] shows that the formula (2.5) is a quite good approximation except at the low-energy end of the spectrum. The most important modification to our discussion of the muon decay comes from the effect of the radiative correction. Some parts of this effect have been studied in previous works.[4] But the radiative correction to the electron polarization in muon decay has not yet been explored.

---

[25] T. Kinoshita and A. Sirlin (unpublished).

π^--Proton Interactions at 5 Bev*†

GEORGE MAENCHEN, WILLIAM B. FOWLER, WILSON M. POWELL, AND ROBERT W. WRIGHT
Radiation Laboratory and Department of Physics, University of California, Berkeley, California
(Received July 10, 1957)

The interaction of 5-Bev negative pions with protons has been studied by exposing a 36-atmosphere hydrogen-filled diffusion cloud chamber to π^- beams from the Berkeley Bevatron. One hundred and thirty-seven interactions producing charged outgoing particles were observed. Of these, 27 were elastic scattering events, 64 were inelastic collisions having two charged outgoing prongs, 39 had four prongs, 3 had six prongs, and 4 involved the production and visible decay of heavy unstable particles. The total cross section is estimated to be 22.5 ± 2.4 mb. The elastic scattering cross section is 4.7 ± 1.0 mb. The angular distribution of the elastic events is consistent with that expected for diffraction scattering from a sphere with radius $(0.9\pm0.15)\times10^{-13}$ cm and opacity 0.6. Analysis of the inelastic events shows that multiple, rather than single, pion production is the predominant process occurring at this energy. An average of 2.3 secondary pions were produced in the inelastic events. This average multiplicity can be fitted by the Fermi statistical theory only by increasing the interaction radius occurring in the theory by 20%. The statistical theory, however, fails to account for the rather marked asymmetry found in the c.m. angular distributions of some of the particles emitted in inelastic events. A combination of the four observed strange-particle production events with 11 similar events obtained in exposures to high-energy neutron and proton beams shows that pion emission accompanies strange-particle production in at least 60% of elementary-particle collisions at Bevatron energies.

I. INTRODUCTION

THIS paper reports a study of π^--p interactions at 5 Bev. Some preliminary reports on this experiment[1] and on the related cloud chamber experiments on $n-p$ and $p-p$ collisions[2,3] at Bevatron energies have already been published.

Investigations of pion-nucleon interactions have tended to fall into several categories according to the range of pion energy. The many experiments at energies up to about 250 Mev have yielded detailed information on elastic scattering and could be analyzed in terms of phase shifts. At higher energies inelastic processes become important and the number of possible angular-momentum states increases. Consequently a phase-shift analysis is no longer feasible. The energy dependence of the total cross section has been measured,[4] and the elastic and inelastic processes in the 1- to 1.5-Bev range have been studied by use of nuclear emulsions[5] and hydrogen-filled diffusion cloud chambers.[6]

Upon successful operation of the Berkeley Bevatron,

---

[1] Maenchen, Powell, Saphir, and Wright, Phys. Rev. **99**, 1619 (1955); Maenchen, Fowler, Powell, Saphir, and Wright, Phys. Rev. **100**, 1802 (1955); Fowler, Maenchen, Powell, Saphir, and Wright, Phys. Rev. **103**, 208 (1956); Maenchen, Fowler, Powell, and Wright, Bull. Am. Phys. Soc. Ser. II, **1**, 386 (1956).

[2] Fowler, Maenchen. Powell Saphir, and Wright, Phys. Rev. **101**, 911 (1956); Holmquist, Fowler, and Powell, Bull. Am. Phys. Soc. Ser. II, **1**, 392 (1956).

[3] Wright, Saphir, Powell, Maenchen, and Fowler, Phys. Rev. **100**, 1802 (1955); Wright, Powell, Maenchen, and Fowler, Bull. Am. Phys. Soc. Ser. II, **1**, 386 (1956).

[4] Cool, Piccioni, and Clark, Phys. Rev. **103**, 1082 (1956).

[5] W. D. Walker and J. Crussard, Phys. Rev. **98**, 1416 (1955); Walker, Hushfar, and Shephard, Phys. Rev. **104**, 526 (1956).

[6] Eisberg, Fowler, Lea, Shephard, Shutt, Thorndike, and Whittemore, Phys. Rev. **97**, 797 (1955).

it became possible to extend these measurements to considerably higher energies. The total cross section for π^--p collisions as a function of energy has been measured,[7] and several studies of the interaction of pions in emulsion have been made.[8]

In the experiment presented here π^--p interactions were observed in a hydrogen-filled diffusion cloud chamber exposed to 4.5- and 5.0-Bev pion beams. The experiment is very similar to the Brookhaven cloud-chamber experiment at 1.4 Bev[6] except that multiple, rather than single, pion production is the predominant process occurring at 5 Bev.

The experiment was intended as a survey of π^--p interactions at Bevatron energies to provide some information on:

(a) Total cross section and the ratio of elastic to inelastic collisions.

(b) Angular distribution of elastic scattering. If the scattering is predominantly diffraction scattering, it may yield information concerning the size and opacity of the proton.

(c) Multiplicity of pion production. The relative frequencies of single, double, triple, and higher pion production could be compared with the predictions of the statistical theories of pion production. If the exact number of secondary pions in each collision could not be determined, owing to the emission of several neutral pions, a lower limit could still be found from the number of charged particles emitted.

(d) Momentum and angular distributions of secondary particles from inelastic collisions.

(e) Possible correlations between pairs of emitted particles.

(f) Production of heavy unstable particles.

II. EXPERIMENTAL PROCEDURE AND REDUCTION OF OBSERVATIONS

A. Apparatus

The observations were made with a diffusion cloud chamber filled with hydrogen at a pressure of 35 atmospheres, with methyl alcohol as condensable vapor. The sensitive region of the chamber was approximately 12 inches in diameter and 2.3 inches high. The chamber was operated in a pulsed magnetic field of 21 500 gauss. An automatic motor-driven camera was mounted directly on the cloud chamber 30 inches above the sensitive volume. Stereoscopic pairs of photographs of the chamber were taken through two 50-mm Leitz Summitar lenses, and a third lens viewed a number register and an ammeter which indicated the current in

[7] N. Frederick Wikner, University of California Radiation Laboratory Report UCRL-3639, January, 1957 (unpublished).
[8] J. O. Clarke and J. V. Major, Phil. Mag. **2**, 37 (1957); Fry, Schneps, and Swami, Phys. Rev. **101**, 1526 (1956); Schein, Haskin, and Glasser, Nuovo cimento **3**, 131 (1956).

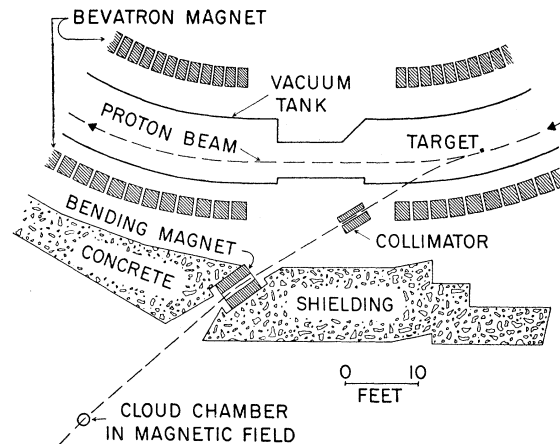FIG. 1. Experimental arrangement.

the magnet. Details of the cloud chamber[9] and the magnet[10] have been described elsewhere.

B. Pion Beam

Pion beams of 4.5 and 5.0 Bev/c were used in this experiment. The 4.5-Bev/c beam was used in the early runs when the maximum proton energy available in the Bevatron was 5.75 Bev. When this proton energy was raised to 6.2 Bev the pion beam geometry was modified slightly to yield 5.0-Bev/c pions. About 75% of the data were obtained in the 5-Bev/c beam. The 4.5- and 5.0-Bev/c data have been lumped together.

The mesons were produced at a target inside the Bevatron and underwent momentum analysis by deflections of 17.6° in the magnetic field of the Bevatron and 10.8° in an external analyzing magnet. A 4-foot-long steel collimator with an aperture 5 inches wide by $\frac{1}{2}$ inch high was inserted between the Bevatron and the analyzing magnet. A plan view of this arrangement is shown in Fig. 1. Various target materials (carbon, uranium, and beryllium) were used during the various runs. In most of the runs an additional 6-foot-long steel collimator with a vertical aperture of 1 inch and no sides was placed between the analyzing magnet and the cloud chamber. This collimator limited the height of the beam in the chamber but did not contribute to momentum selection. Both collimators were slightly wider at their exit ends to minimize slit scattering.

The momenta of several groups of beam tracks in the cloud chamber were determined by measuring the curvatures of the beam tracks with a micrometer-stage microscope. The resulting pion-momentum spectra are shown in Fig. 2. These measurements yielded momenta of 4.49 ± 0.30 and 4.99 ± 0.33 Bev/c, where the uncertainty of the *average* momentum in each group is about ±0.05 Bev/c. Pion trajectories were plotted to

[9] Elliott, Maenchen, Moulthrop, Oswald, Powell, and Wright, Rev. Sci. Instr. **26**, 696 (1955).
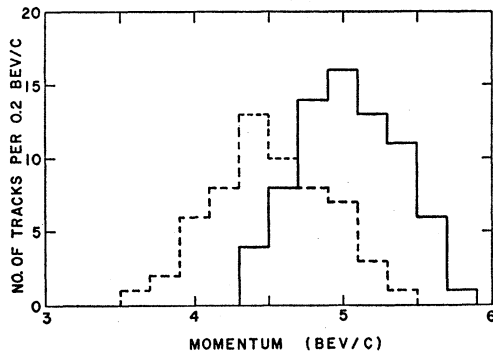[10] W. M. Powell, Rev. Sci. Instr. **20**, 403 (1949).

FIG. 2. Distributions of measured momenta of π^--beam tracks. The dashed lines refer to the early run at a mean pion momentum of 4.49 Bev/c. The solid lines represent the distribution from the later runs at a mean pion momentum of 4.99 Bev/c.

determine the expected beam momentum, with results in excellent agreement with the cloud chamber values. The plotted trajectories indicated a momentum spread of about ±0.25 Bev/c. The somewhat larger momentum spread observed in the chamber is presumably due to errors of measurement, discussed in Sec. II-D, and to scattering of pions from the collimators. Because the latter effect was ignored in the plotted trajectories, the more conservative values found from curvature measurements in the cloud chamber were used for the pion momentum in processing the events.

C. Scanning

About 15 500 photographs were obtained. They were scanned for deflections or interactions of beam tracks and also for V-particle decays. As the total charge of the π^--p system is zero, all hydrogen events must have an even number of emergent prongs, half positive and half negative. The events were classified as 2-, 4-, or 6-prong events. No π^--p collisions resulting in more than six charged outgoing particles were observed. Zero-prong events were searched for, but because they showed no charged outgoing particles it was extremely difficult to distinguish them from tracks leaving the sensitive region or entering gaps. Only one certain example of such an event was found. All the film was scanned at least twice and most of it three times. Scanning efficiencies e_1 and e_2 for two scanners may be defined by

$n_1 = e_1 N = $ No. of events found by scanner No. 1,
$n_2 = e_2 N = $ No. of events found by scanner No. 2,
$n_{12} = e_1 e_2 N = $ No. of events found by scanners No. 1 and No. 2

(where N is the true number of events). We find $e_1 = 0.80$ and $e_2 = 0.90$, and a combined efficiency for double scanning $1 - (1 - e_1)(1 - e_2) = 0.98$. All the film was scanned by these two scanners and most of it was scanned a third time by a more experienced scanner; the over-all scanning efficiency is probably greater than 98%.

D. Measurements

Of the events found by scanning, only those satisfying certain selection criteria, described in Sec. III-A, were considered for further analysis. The events were measured on a stereoscopic projector.[11] The projector duplicates the optical system of the camera and permits the reconstruction, in space, of events that occurred within the chamber. For each event the film number, x, y, z position of the origin, magnet current, and number of prongs were recorded. For each track the following information was recorded:

(a) Radius of curvature ρ and the estimated uncertainty $+\Delta\rho_+$, $-\Delta\rho_-$. The $\Delta\rho_+$ was generally larger than $\Delta\rho_-$. Radii were usually measured with ruled templates, although occasionally a micrometer-stage microscope was used. The uncertainty in ρ arises from an uncertainty in the sagitta. For most tracks the sagitta could be measured to ±0.05 mm. Abnormally dense or diffuse tracks had sagitta uncertainties two to five times as large.

(b) Dip angle α between the track and its projection in the horizontal plane, and the estimated uncertainty $\pm\Delta\alpha$. (Typically $\Delta\alpha \simeq 1.0°$.)

(c) Azimuthal angle β between the horizontal projection of the track and the direction of the pion beam and the estimated uncertainty of β. Typically $\Delta\beta \simeq 0.5°$.

(d) The estimated ionization density dE/dx and its uncertainty.

(e) The visible length of the track.

(f) The height and horizontal distance from the magnet centerline of the center of the track (for determining the effective magnetic field).

(g) Identification of the track. When the momentum and ionization of a positive track were such as to definitely identify it as a pion or a proton this fact was noted. All negative tracks were assumed to be pions.

In order to eliminate gross measurement errors, each event was independently measured at least twice. The results were then compared, and if a discrepancy was found the event was remeasured. If the agreement was satisfactory, either the measurements were averaged or the measurement by the most experienced person was used. From a comparison of repeated measurements on a sample of about 50 tracks it was found that the estimated uncertainties mentioned above correspond to approximately 1.25 standard deviations for angle measurements and 1.5 standard deviations for radius-of-curvature measurements.[12]

The accuracy of momentum measurements is inversely proportional to the momentum. The incident-pion track was therefore the most poorly measured track in most events. Consequently the momentum of

[11] Brueckner, Hartsough, Hayward, and Powell, Phys. Rev. 75, 555 (1949).
[12] B. H. Armstrong, University of California Radiation Laboratory Report UCRL-3470, July, 1956 (unpublished).

the incident pion was assumed to be that of the average beam particle, as determined by the spectrum measurements described above.

Errors due to gas motion (as determined from measurements on beam particles with the magnet turned off) were quite small, and contributed a spurious radius of curvature that, in the worst cases, was still more than 50 meters. This error is much smaller than the normal measurement uncertainties, and was usually neglected. Photographs, taken with the same optical system, of ruled grids of straight lines indicated that optical distortion was negligible.

E. Data Reduction and Classification of Events

In most of the inelastic events one or more neutral particles were emitted. These neutral particles carried off momentum P_N and energy E_N. Information on the presence and, in some cases, the number of neutral particles may be obtained from the requirement that energy and momentum be conserved in the event. In an inelastic event having $n(=2, 4,$ or $6)$ charged outgoing particles whose momenta and angles have been measured, the mass M_N of a single neutral particle can be calculated by

$$M_N = (E_N{}^2 - P_N{}^2)^{\frac{1}{2}},$$

$$E_N = E_0 + M_p - \sum_{i=1}^{n} E_i,$$

$$\mathbf{P}_N = \mathbf{P}_0 - \sum_{i=1}^{n} \mathbf{P}_i,$$

TABLE I. Classes of events considered in this paper.

Type	Charge state[a]	Number of secondary pions, m	Mass of neutral particle, M_N (Mev)
Zero-prong	$(n0)$	0	
(not recorded)	$(n00\cdots)$	$\geqslant 1$	
Elastic 2-prong	$(p-)$	0	0
Inelastic:			
2-prong	$(p-0)$	1	135
	$(n+-)$	1	940
	$(p-00\cdots)$	$\geqslant 2$	$\geqslant 270$
	$(n+-0\cdots)$	$\geqslant 2$	$\geqslant 1075$
4-prong	$(p+--)$	2	0
	$(p+--0)$	3	135
	$(n++--)$	3	940
	$(p+--00\cdots)$	$\geqslant 4$	$\geqslant 270$
	$(n++--0\cdots)$	$\geqslant 4$	$\geqslant 1075$
6-prong	$(p++---)$	4	0
	$(p++---0)$	5	135
	$(n+++---)$	5	940

[a] The notation $(p-00\cdots)$ means that one proton, one π^-, and two neutral pions resulted from the collision. The notation $\cdots$ is used to indicate the possibility of additional neutral pions. The ordering of the pions is of no significance.
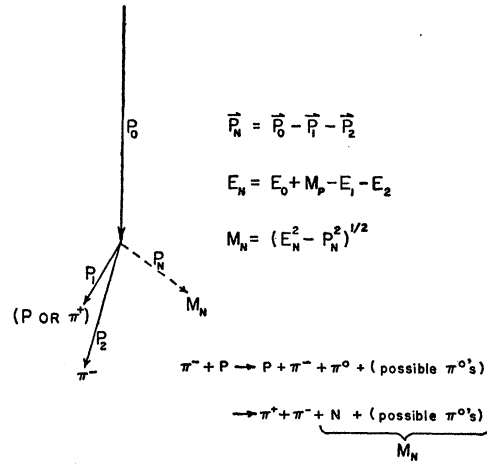

$$\vec{P}_N = \vec{P}_0 - \vec{P}_1 - \vec{P}_2$$

$$E_N = E_0 + M_p - E_1 - E_2$$

$$M_N = (E_N{}^2 - P_N{}^2)^{1/2}$$

$$\pi^- + P \rightarrow P + \pi^- + \pi^0 + (\text{possible } \pi^0\text{'s})$$

$$\rightarrow \pi^+ + \pi^- + N + (\text{possible } \pi^0\text{'s})$$

FIG. 3. Schematic drawing of a typical inelastic 2-prong event.

where E_0, P_0 are the total energy and momentum of the incident π^-, M_p is the mass of the struck proton, and E_i, P_i are the total energy and momentum of the ith outgoing track. A typical inelastic event is shown schematically in Fig. 3. The missing energy, E_N, depends on the masses chosen for the charged outgoing particles. These were all assumed to be pions, with the reservation that one positive track could be a proton. The possibility that some of the outgoing tracks might be K particles or hyperons was ignored except in the very few cases in which visible decays occurred. In about half of the events the positive prongs could be identified as protons or pions by ionization or, in a few cases, by the fact that a proton cannot be emitted from inelastic events at angles greater than about $80°$. When such an identification could not be made the neutral mass was calculated for all the possible mass combinations.

The magnitude of M_N furnishes a clue to the number of neutral particles emerging from a collision but does not, in most cases, specify this number uniquely. Table I lists the types of events that can, in principle, be recognized. For example, an inelastic 2-prong event having an identified proton may have one or more neutral pions. If $M_N = 135$ Mev or can be brought to this value by adjusting the angle and momentum measurements within their errors, then $(p-0)$ is a possible interpretation of the event. If M_N cannot be increased above 270 Mev then $(p-0)$ is the only possible reaction. In this case the adjusted values of momenta and angles that gave M_N exactly equal to 135 Mev are used in the momentum and angular distributions in Sec. III-D. If, on the other hand, M_N cannot be reduced below 270 Mev, then two or more neutral pions were emitted: $(p-00\cdots)$. Two neutral particles of mass M_1 and M_2 and total energy E_1 and E_2 can yield any value of M_N between (M_1+M_2) and (E_1+E_2). Therefore a large value of M_N does not permit us to determine the exact

number of neutral particles. For instance, a value of $M_N = 600$ Mev could be due to 2, 3, or 4 pions.

In the Brookhaven study of 1.4-Bev $\pi^- - p$ collisions it was assumed that the frequency of events involving the production of three or more secondary pions was negligible.[6] This made it possible, in principle, to classify each event uniquely, because any event having two charged prongs could have no more than two neutral particles. In our experiment, examples of quadruple pion production were observed. Consequently the unique classification of 2-prong (and 4-prong) events is no longer possible.

These calculations of M_N were carried out on an IBM 650 computer. When the positive particles were not identified the machine tried all combinations consistent with the number of prongs and the reactions in Table I. Thus in a 4-prong event there are three possible choices in assigning masses to the measured tracks: $p + - -$, $+ p - -$, and $+ + - -$. For each permitted choice the machine calculated P_N, E_N, M_N, and the derivatives of M_N with respect to all the input parameters: P_0, P_1, P_2, $\cdots$, α_1, α_2, $\cdots$, β_1, β_2, $\cdots$. Then, using these derivatives, it used an iterative procedure to find the amount of adjustment of the input data (within the estimated errors) necessary to bring M_N to values corresponding to the appropriate neutral particle. In this adjustment each parameter was varied in proportion to its uncertainty. The amount of adjustment τ is defined by $\tau = |x_\tau - x_0| / \Delta x$, where x is any of the input parameters, Δx is the estimated uncertainty of x (in the direction of the adjustment), x_0 is the measured value, and x_τ is the value used in the adjusted solution. The maximum and minimum values of M_N, corresponding to $\tau = \pm 1$, were also calculated. The magnitude of τ served as a measure of the probability that the corresponding adjusted solution is indeed the correct one. For example, an event having an unadjusted ($\tau = 0$) $M_N = 1$ Bev and requiring a τ of -0.95 to fit the ($p - 0$) reaction would be classed as $(p - 00 \cdots)$, because an adjustment of all the input parameters by 95% of their errors is extremely improbable.

In most events, however, the main variation in M_N is generally due to only a few of the input parameters (usually the momenta). Although all the measured quantities were adjusted, some had such small errors (or small $\partial M_N / \partial x$) that almost the same adjustment of only a few parameters would have yielded the same value of M_N. Consequently the probability that a given adjustment is the correct one depends not only on τ but also on the number of input parameters that strongly affect M_N. This number is much smaller than the total number of input parameters, and is usually 2, 3, or 4. Since the estimated errors of the momentum measurements correspond to about 1.5 standard deviations, an adjustment of two momenta by 65% of their errors corresponds to a probability of about 5%. A 65% adjustment of three parameters yields a probability of

only 0.3%. Therefore only those adjusted solutions having $\tau < 0.65$ were considered as valid possibilities.

For each solution, adjusted or unadjusted, the machine also calculated the laboratory polar angles θ and ϕ, the c.m. (center-of-mass) angle θ^*, and the c.m. momentum p^* for each particle, as well as Q values and c.m. correlation angles between all pairs of particles. The average time required for one adjusted solution, including calculation of all the c.m. quantities, was approximately 2 minutes.

III. RESULTS AND DISCUSSION

A. Total Cross Section

The sensitive region of the chamber had occasional insensitive gaps due to local depletion of methanol vapor. Because $\pi^- - p$ collisions occurring in such gaps might be missed in scanning, only those events satisfying the following selection criteria were used for finding the total cross section: The origin of the event must be clearly visible in both stereoscopic views and must be located in a well-defined 10-by-10-inch fiducial region in the chamber[13]; the momentum of the incident pion must be consistent with the beam momentum, and its direction must be within $\pm 4°$ of the average beam direction.

In order to find the total cross section the flux of pions must be known. The visible length of beam tracks was measured in every 25th picture by use of these same selection criteria. The average temperature of the gas at the level of the beam was $-40 \pm 5°C$, and the average pressure was 519.4 psig. From the average track length per picture and the total number of pictures taken, the total track length was found to be 11 600 g/cm² of H_2. Despite the large distance from the Bevatron target to the chamber, the high momentum ($\beta\gamma \simeq 35$) yields the rather low calculated μ^- contamination of $5 \pm 2\%$.

A total of 130 events was found under the above restrictions. This includes four events involving production of heavy unstable particles. The probability that any of these events is due to collisions with carbon or oxygen nuclei is considered extremely small. Methyl alcohol, which was the condensable vapor in the cloud chamber, constituted about 0.1% of the gas molecules at the beam level. Carbon or oxygen stars should be recognizable as such because of the net positive charge of the event of 5 or 7, and because of the typical highly ionizing low-momentum prongs. Assuming a cross section of $(60)A^{\frac{2}{3}}$ mb, we expect to find two π^--alcohol collisions. The three alcohol stars observed were easily recognized.

To find the total cross section the following corrections must be applied. The scanning efficiency (Sec. II-C)

---

[13] Seven additional events with origins near the entrance end of the chamber but slightly outside the fiducial region were included in the distributions in Secs. III-B through III-E, but were not included in the calculation of the total cross section.

was estimated at 98%. The angular distribution of elastic events (Sec. III-B) indicated that 8 ± 4 small-angle elastic events were missed. This type of missed event is in addition to the scanning-efficiency correction. These corrections yield a cross section for all processes involving charged secondary particles of

$$\sigma_{\text{charged}} = 21.1 \pm 2.3 \text{ mb.}$$

The total cross section is slightly larger than this because those events in which all the outgoing particles are neutral were not recorded. These unrecorded zero-prong events may be divided into elastic ($n0$) and inelastic ($n00\cdots$) events. The number of inelastic zero-prong events is estimated to be nine (see Sec. III-C). This estimate is based on charge-independence considerations and on the number and type of observed inelastic events. It is somewhat dependent on the relative frequency of π^--p interactions in the isotopic spin $T = \frac{3}{2}$ and $\frac{1}{2}$ states. In this experiment, in which double and triple pion production is frequent, the number of inelastic zero-prong events is small and rather insensitive to the $T = \frac{3}{2}, \frac{1}{2}$ mixture.

The number of charge-exchange ($n0$) events, however, depends strongly on the relative strength of interaction in these two isotopic spin states.[14] For $\sigma_{\frac{3}{2}} = \sigma_{\frac{1}{2}}$ the predicted ratio ($n0$): ($p-$) is 0:1; it is 2:1 for $\sigma_{\frac{1}{2}} = 0$, and 1:2 for $\sigma_{\frac{3}{2}} = 0$. Assuming for the moment that we have $\sigma_{\frac{3}{2}} \simeq \sigma_{\frac{1}{2}}$, so that there is very little charge-exchange scattering, we find that the total cross section is

$$\sigma_{\text{total}} = 22.5 \pm 2.4 \text{ mb.}$$

This cross section may be compared with the total cross sections at 4.3 Bev/c found by Wikner[7] in a good-geometry attenuation experiment. He finds $\sigma(\pi^-,p) = 28.7 \pm 2.6$ mb and $\sigma(\pi^-, D_2O - H_2O) = 23.0 \pm 2.6$ mb. From the latter, one may apply a correction of 5 ± 2 mb for the "shadow effect,"[4] and find $\sigma(\pi^-,n) = 28 \pm 4$ mb. The near equality of the π^--p and π^--n cross sections, obtained in the same experiment, indicates that $\sigma_{\frac{3}{2}}$ and $\sigma_{\frac{1}{2}}$ are nearly equal and that consequently the charge-exchange cross section is very small. A similar result was found by Cool et al.[4] at 2 Bev/c. Therefore the slightly low cross section found in our experiment is presumably not due to a failure to count charge-exchange events.

If, on the other hand, the 6.2-mb difference between the total π^--p cross sections measured by Wikner and by us were due to charge-exchange scattering, then the measured elastic cross section of 4.7 mb (Sec. III-B) would imply that the ratio of the scattering amplitudes in the $T = \frac{3}{2}$ and $\frac{1}{2}$ states is about 14:1 (if the phases are about the same). This ratio would require a π^--n elastic cross section of about 32 mb, which is clearly incompatible with Wikner's measured total π^--n cross section of 28 mb, most of which is probably inelastic. It must be concluded that the difference between these two
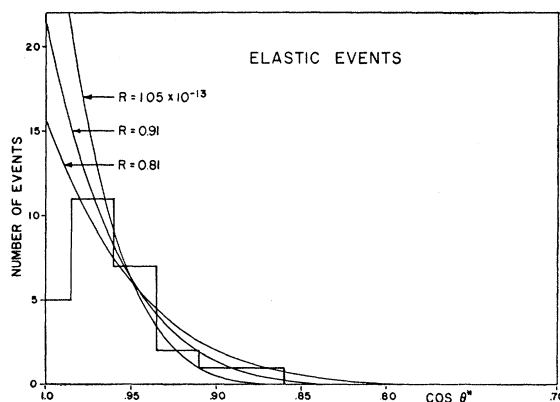

FIG. 4. Center-of-mass angular distribution of elastic events.

measurements of the π^--p total cross section is due to statistical fluctuations and perhaps to systematic errors, and not, in the main, to charge-exchange scattering. We have not found any systematic errors that could account for this difference.

B. Elastic Events

The most easily identified events were the elastic scatters. They can be recognized by three independent criteria: the incident and outgoing tracks are coplanar, the laboratory angles of the outgoing tracks are simply related, and the momentum of each outgoing track is related to its angle. In practice the last criterion was used only as a check, because the angle measurements were always more precise than the momentum measurements.

Only 27 elastic events were observed. Their angular distribution in the c.m. system is shown in Fig. 4. The distribution obviously suggests that the elastic events are due to diffraction scattering—which, indeed, is to be expected as a consequence of the inelastic interactions.[15] Two of the events occurred at large angles far outside the diffraction pattern, and are considered in the next section.

In this experiment the wavelength of the incident pion in the c.m. system is considerably smaller ($\lambda \simeq 1.4 \times 10^{-14}$ cm) than the size of the proton ($\approx 10^{-13}$ cm) as defined by the range of nuclear forces or by its spatial charge distribution.[16] One may therefore attempt to describe the diffraction scattering by methods commonly applied to nuclei.[17] The statistics are far too poor to justify an attempt to distinguish between various proton density distributions, but it is of interest to fit the data with the diffraction scattering from a uniform opaque or semitransparent sphere of radius R. Curves of the expected distribution for three values of R

[14] H. A. Bethe and F. deHoffman, *Mesons and Fields* (Row, Peterson, and Company, Evanston, 1955), p. 62.

[15] J. M. Blatt and V. F. Weisskopf, *Theoretical Nuclear Physics* (John Wiley and Sons, Inc., New York, 1952), Chap. VIII.
[16] E. E. Chambers and R. Hofstadter, Phys. Rev. **103**, 1454 (1956).
[17] Fernbach, Serber, and Taylor, Phys. Rev. **75**, 1352 (1949); H. A. Bethe and R. R. Wilson, Phys. Rev. **83**, 690 (1951).

TABLE II. Comparison of interaction radii found by several experiments.

System	Bombarding energy (lab) (Bev)	Interaction radius (10^{-13} cm)	Opacity	Reference
π^--p	5.0	0.9	0.6	(this experiment)
π^--p	1.4	1.2	0.6	c
$p-p$	4.4	1.0[a]		d
$p-p$	2.75	0.93	0.92	e
$p-p$	1.5	0.93	0.96	e
$p-p$	0.81	0.93	0.97	e
e^--p	0.2–0.5	0.77[b]		f

[a] Rms radius of region of pure absorption. In addition to this, the data appear to indicate a region of potential interaction of rms radius 0.45 $\times10^{-13}$ cm.
[b] Rms radii of the charge and moment distributions.
[c] See reference 6.
[d] W. A. Wenzel (private communication).
[e] W. B. Fowler et al., Phys. Rev. 103, 1489 (1956).
[f] See reference 16.

are shown in Fig. 4. A radius of $R=(0.9\pm0.15)\times10^{-13}$ cm fits the data quite well, and indicates that about 8 ± 4 small-angle events (corresponding to laboratory angles of less than 3°) were missed in scanning the film. The cross section has been corrected for these missed events, and may be separated into diffraction $\sigma_d=4.7$ mb and reaction $\sigma_a=17.7$ mb. This yields an opacity $\sigma_a/\pi R^2=0.6\pm0.2$ and an absorption coefficient $K=1.02\times10^{13}$ cm^{-1}, and fits Bethe and Wilson's curve for $k_1\lambda\simeq0$ (here k_1 depends on the nuclear potential and λ is the mean free path in nuclear matter). The comparisons in Table II show that these values are similar to the interaction radii and opacities found in other experiments.

C. Inelastic Events

Eighty percent of the events were inelastic and involved pion production. The data-reduction process described in Sec. II-E was used to classify these events, as far as possible, according to the charge states listed in Table I. In about half the events the charge state of the nucleon (i.e., whether it was emitted as a proton or as a neutron) could not be determined. In ten of these events it was possible, however, to determine that two or more neutral particles were emitted regardless of the charge state of the nucleon, so that some information about multiplicity of pion production could be obtained although the exact charge state was not known. The classification of all events is given in Table III.[18]

One of the objectives of the experiment was to obtain some information about the relative frequency of single, double, triple, and higher pion production. The classifications listed in Table III do not provide this information directly because for many events only the lower limit of multiplicity can be specified. Thus an event classed as $(p-00\cdots)$ can involve the production of 2, 3, 4, or 5 pions. However, by use of the principle of charge

[18] One of the events listed in the 4-prong group in Table III actually had six charged prongs, two of which were electrons. These electrons were presumably due to a $\pi^0\rightarrow e^++e^-+\gamma$ decay.

independence, information about the multiplicities can be obtained from the distribution of the events in Table III. Here we assume that the probability of observing a system of one nucleon and a given number of pions in its various possible charge states is proportional to the statistical weight[19] of each charge state. These statistical weights are essentially just the Clebsch-Gordan coefficients relating the isotopic spin states to the various charge states.

Table IV lists the statistical weights used in analyzing the event distribution. It was calculated with the assumption $\sigma_{\frac{3}{2}}\simeq\sigma_{\frac{1}{2}}$ (see Sec. III-A). The statistical weights for the inelastic processes are rather insensitive to the $\frac{3}{2}$, $\frac{1}{2}$ mixture. The entries in Table IV are the normalized probabilities that an event involving the production of m pions appear as an n-prong star. For example: a double pion-production event has a 28% probability of showing four charged prongs $(p+ - -)$; 66% of having two charged prongs: $(p-00)$ or $(n+ -0)$; and 6% of showing no charged prongs $(n000)$ and thus not being recorded. For every $(p+ - -)$ event observed there must be, on the average, 66/28 inelastic 2-prong events involving double pion production and 6/28 unrecorded zero-prong events. These statistical weights may be used to find a set of cross sections for various multiplicities of pion production that is consistent with the event distribution shown in Table III. Unfortunately such a set of cross sections is not unique. Consequently several such sets, all of them consistent with the data, were calculated, so as to

TABLE III. Classification of events.

Type	Charge state	No. of events	Multiplicity m
Elastic nondiffraction	$(p-)$	2	0
Inelastic 2-prong (64 events)	$(p-0)$ $3\}$ $(n+ -)$ $3\}$	6	=1
	uncertain	30	$\geqslant1$
	$(p-00\cdots)$ $8\}$ $(n+ -0\cdots)$ $11\}$ $(p-00\cdots)$ or $(n+ -0\cdots)$ $9\}$	28	$\geqslant2$
4-prong (39 events)	$(p+ - -)$	8	=2
	uncertain	5	$\geqslant2$
	$(p+ - -0)$ $1\}$ $(n+ + - -)$ $2\}$	3	=3
	uncertain but not $(p+ - -)$	18	$\geqslant3$
	$(n+ + - -0\cdots)$ $4\}$ $(p+ - -00\cdots)$ or $(n+ + - -0\cdots)$ $1\}$	5	$\geqslant4$
6-prong (3 events)	$(p+ + - - -)$ $1\}$ uncertain $1\}$ $(n+ + + - - -)$ $1\}$	3	$\geqslant4$
Diffraction elastic $(p-)$[a]		33	
Strange-particle production		4	

[a] Corrected for missed small-angle events.

[19] R. H. Milburn, Revs. Modern Phys. 27, 1 (1955).

give some indication of the variations allowed by the data. The following sample calculation illustrates the process.

It is assumed throughout that production of more than five pions does not occur, because only three 6-prong and no 8-prong events were observed. Let n_m be the number of collisions in which m new pions were produced. Because the number of 6-prong events observed was 3, we have $(0.129)n_4 + (0.342)n_5 = 3$, that is, 12.9% of the quadruple pion production events result in six charged prongs (see Table IV). We may thus choose any trial value of n_5 between 0 and 9. If we choose $n_5 = 3$, the number of observed 6-prong events requires that $n_4 = (3 - 0.342n_5)/0.129 = 15$. From Table IV we find that $(0.543)n_5 + (0.639)n_4 = 11.2$ of the 4-prong events and $(0.112)n_5 + (0.224)n_4 = 3.7$ of the 2-prong events were due to n_4 and n_5. Subtracting these from the distribution in Table III, one finds a reduced distribution which involves only single, double, and triple production. One now repeats the process, choosing some reasonable value for n_3, finding the value of n_2 required to account for all the remaining 4-prong events, finding the number of 2-prong events due to n_2 and n_3, and finding the value of n_1 that will account for all the remaining inelastic 2-prong events. In all cases $n_0 = 2/0.556 \simeq 4$, since it must account for the two wide-angle elastic events. In this way one can rapidly find many sets of n_m that fit the data. Several such sets are shown in Fig. 5. The smooth curves in Fig. 5 are intended only to guide the eye from one point to the next. Some of the sets of points involve a dip at n_2 or at n_4 and are considered rather unlikely. About 20 sets of n_m were calculated, for some of which slight variations of the distribution of Table III were used to test the effect of the statistical uncertainties in the data. Although the "curves" for the various sets differed greatly in appearance they all yielded nearly the same values for the total number of reaction collisions, $\sum_m n_m = 117$, and for the average number of pions produced per collision, $\bar{m} = \sum_m m n_m / \sum_m n_m = 2.3 \pm 0.1$ (these numbers do not include the four events involving production of heavy unstable particles). The total number of reaction collisions indicates that nine reaction events involving no charged outgoing prongs occurred. The total cross section (Sec. III-A) has been corrected for these unrecorded events.
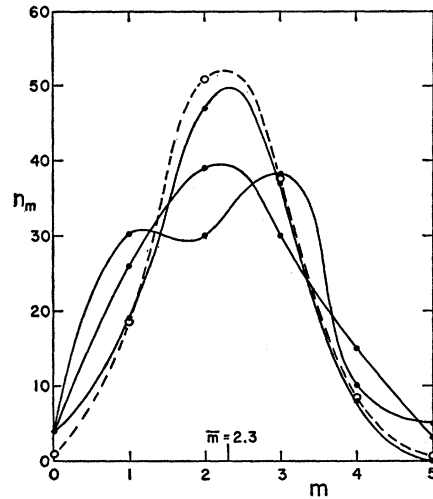

FIG. 5. Three possible sets of multiplicities. Here n_m is the number of events in which m secondary pions are produced. The solid curves connect sets of points found from the data. The dashed curve connects the set of points predicted by the statistical theory using a modified radius and normalized to a total of 117 events.

Fermi has proposed a statistical theory to describe multiple pion production in high-energy collisions.[20] In this theory and its several modifications[21,22] it is assumed that the initial interacting particles coalesce into a small volume Ω and that this interaction region survives long enough to allow all the possible final states to reach a statistical equilibrium. Thus the probability of observing a particular final state depends only upon the total statistical weight of that state. In all the statistical theories the assumption of statistical equilibrium requires that the angular distribution of the emerging particles be symmetric about 90° in the center-of-mass system. It will be seen in Sec. III-D that some of the distributions are quite asymmetric, indicating that complete statistical equilibrium was not attained in these π^--p collisions. Nevertheless it is of interest to calculate the multiplicities predicted by the Fermi theory and to compare them with the results of this experiment.

In the Fermi theory the probability that one nucleon and $m+1$ pions result from the π^--p collision is

$$P(m) = \text{const}\,(\Omega/h^3)^{m+1} S(m) T(m) dQ/dW.$$

Here Ω is the volume resulting from the Lorentz contraction of a spherical interaction volume $\Omega_0 = (4/3)\pi R^3$. In the Fermi theory the interaction radius R is assumed to be the Compton wavelength of the pion $(R_0 = \hbar/\mu c$

TABLE IV. Probability that n charged prongs emerge from a π^--p collision producing m secondary pions.

No. of outgoing particles	No. of new pions, m	Probability of n charged prongs			
		$n = 0$	2	4	6
2	0	0.444	0.556		
3	1	0.156	0.844		
4	2	0.061	0.662	0.277	
5	3	0.021	0.411	0.568	
6	4	0.008	0.224	0.639	0.129
7	5	0.003	0.112	0.543	0.342

[20] E. Fermi, Progr. Theoret. Phys. (Japan) 5, 570 (1950); Phys. Rev. 92, 452 (1953); Phys. Rev. 93, 1434 (1954).
[21] J. V. Lepore and R. N. Stuart, Phys Rev 94, 1724 (1954); Lepore, Neuman, and Stuart, Phys. Rev. 94, 788 (1954).
[22] S. Z. Belenkii and A. I. Nikishov, J. Exptl. Theoret. Phys. (U.S.S.R) 28, 744 (1955) [translation: Soviet Phys JETP 1, 593 (1955)]; A. I. Nikishov, J. Exptl. Theoret. Phys. (U.S.S.R.) 30, 990 (1956) [translation: Soviet Phys. JETP 3, 783 (1956)].

$=1.4\times10^{-13}$ cm). Because the predicted multiplicity of pion production is a rather sensitive function of R, we treat R as an adjustable parameter. Hence Ω/h^3 may be expressed as

$$\frac{\Omega}{h^3}=\frac{1}{\gamma}\left(\frac{1}{2\pi\hbar}\right)^3\frac{4\pi}{3}\left(\frac{\hbar}{\mu c}\right)^3\left(\frac{R}{R_0}\right)^3=9.117\times10^{-3}\left(\frac{R}{R_0}\right)^3,$$

where γ is the Lorentz contraction factor due to the proton's motion in the c.m. system, and $\mu=c=1$. The factor $S(m)$ takes into account the indistinguishability of the pions, where $S(m)=1/(m+1)!$. The isotopic-spin weight factor $T(m)$ is the number of ways a system of one nucleon and $m+1$ pions can form a state of given total isotopic spin. The factor dQ/dW is the volume in momentum space available to the system subject to the conservation of energy and momentum. It was calculated by means of the saddle-point approximation method of Fialho.[23] This method treats all the particles as exact relativistically but does not provide for conservation of angular momentum and conservation of the "center of energy."[21] Absorbing a constant factor of Ω/h^3 into the constant, we find

$$P(m)=\text{const}\,(9.117\times10^{-3})^m\left(\frac{R}{R_0}\right)^{3m}\frac{T(m)}{(m+1)!}\frac{dQ}{dW}.$$

Table V lists several sets of $P(m)$ corresponding to various choices of R/R_0. The dependence of the average multiplicity, $\bar{m}$, upon R/R_0 is shown in Fig. 6. The experimental value of $\bar{m}=2.3$ corresponds to $R=1.19R_0$ $=1.7\times10^{-13}$ cm. The difference between this value and the interaction radius $(0.91\times10^{-13}$ cm) found from the diffraction pattern of the elastic events may indicate that the interaction volume expands somewhat before the system breaks up into a group of free particles. The set of $P(m)$ corresponding to $R/R_0=1.19$ is shown in Fig. 5 together with some of the possible experimental distributions.
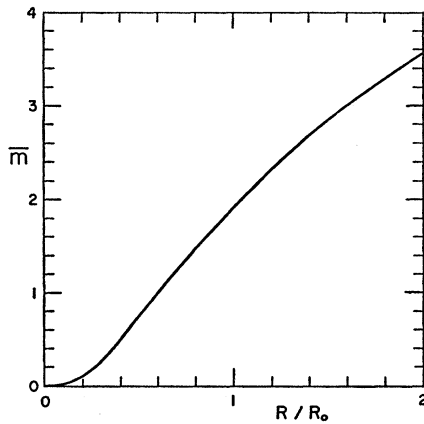
These results may be compared with the multiplicity of meson production in antiproton annihilation. In the Antiproton Collaboration Experiment[24] the annihilation of 35 antiprotons was observed. In these events the available energy in the c.m. system was very nearly the same as in the 5-Bev π-p collisions. The average number of pions per annihilation was estimated in two ways. One method assumes that the average number of neutral pions is one-half the average number (2.6) of charged pions. A 10% correction for detection efficiency was applied and the average number (1.0) of pions absorbed was added; an average multiplicity of 5.3 was found. A second method, using energy conservation and the average energy of the charged pions, assumes that the neutral pions have the same average energy, and yields very nearly the same result. A combination of these two methods yielded an average multiplicity of 5.3 ± 0.4, which is greater than predicted by the Fermi statistical theory. In order to raise the predicted multiplicity to 5.3, the interaction radius must be increased to 2.3 $\hbar/\mu c$.

The inelastic π^--p collisions produced an average of 2.3 secondary pions in addition to the original pion and nucleon, giving a total of 4.3 emitted particles. The absence of a nucleon in the annihilation stars may account for the difference in the number of emitted particles. However, the interaction radius of 2.3 $\hbar/\mu c$ required to account for the average multiplicity in antiproton annihilation is in marked contrast to the radius of 1.2 $\hbar/\mu c$ found in the 5-Bev π^--p collisions. This discrepancy indicates that for one or both of these processes the statistical model, as used here, is not a valid description.

A similar calculation has been done by Nikishov,[22] using a radius of 1.4×10^{-13} cm and a modification of the Fermi theory to include the possibility of forming a $J=T=\frac{3}{2}$ nuclear isobar. Although the pions were treated as extreme relativistic particles in Nikishov's calculation, the results are quite similar to those presented here.

FIG. 6. Predicted average multiplicity, $\bar{m}$, as a function of the ratio of the interaction radius R to the pion Compton wavelength R_0.

[23] G. E. A. Fialho, Phys. Rev. 105, 328 (1957).

TABLE V. Relative probability of producing m secondary pions as predicted by the statistical theory.

Number of secondary pions, m	$P(m)$				
	$R/R_0=0.67$	1.00	1.19	1.50	2.00
0[a]	0.151	0.024	0.008	0.001	0.000
1	0.546	0.284	0.159	0.053	0.008
2	0.266	0.461	0.434	0.290	0.103
3	0.035	0.203	0.321	0.432	0.363
4	0.001	0.027	0.072	0.195	0.389
5	0.000	0.001	0.005	0.028	0.135
$\bar{m}=1.19$		1.93	2.30	2.85	3.54

[a] Does not include diffraction scattering.
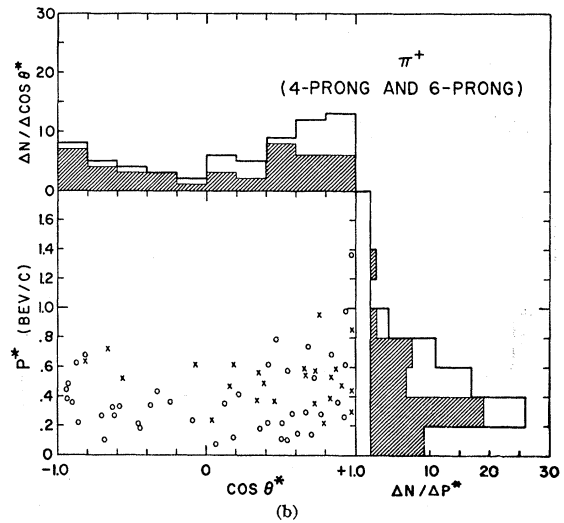
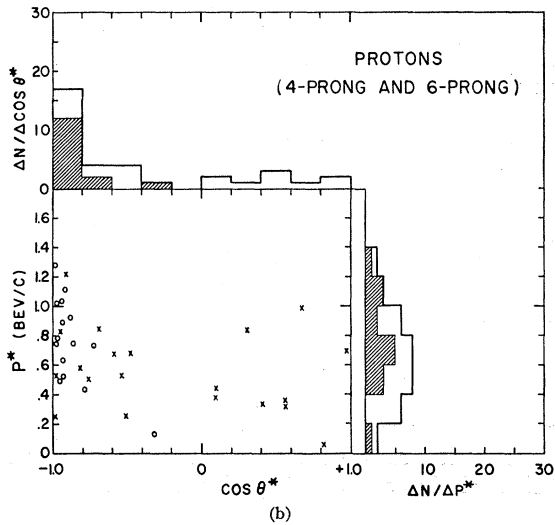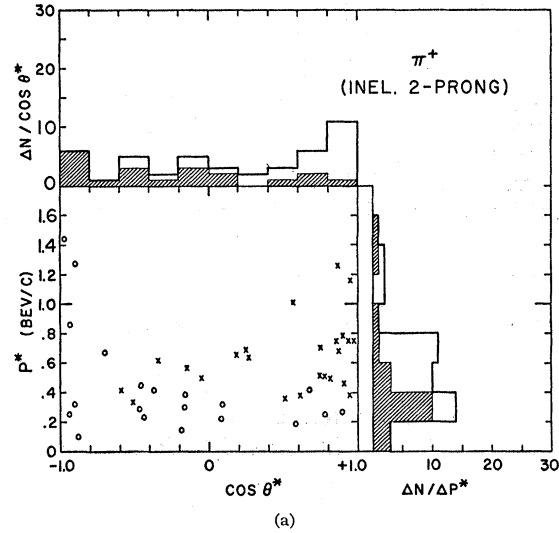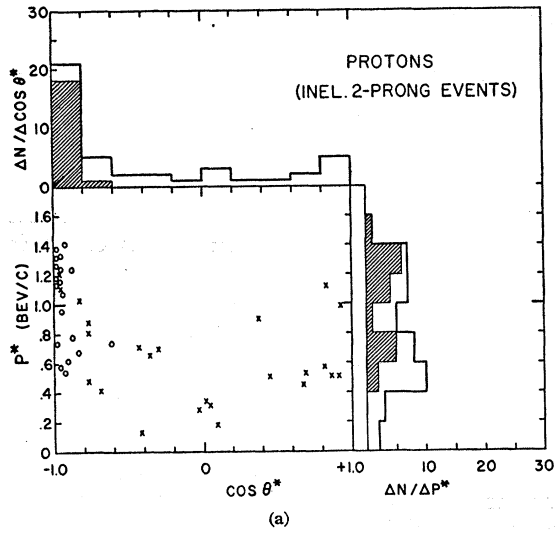[24] W. H. Barkas et al., Phys. Rev. 105, 1037 (1957).

FIG. 7. Center-of-mass scatter diagrams of protons from inelastic 2-prong events (upper) and from 4-prong and 6-prong events (lower). Positive particles definitely identified as protons are represented by circles (o) and the shaded portion of the histograms. Unidentified positive particles (calculated on the basis of a proton mass) are represented by crosses (✕) and by the unshaded portion of the histograms.
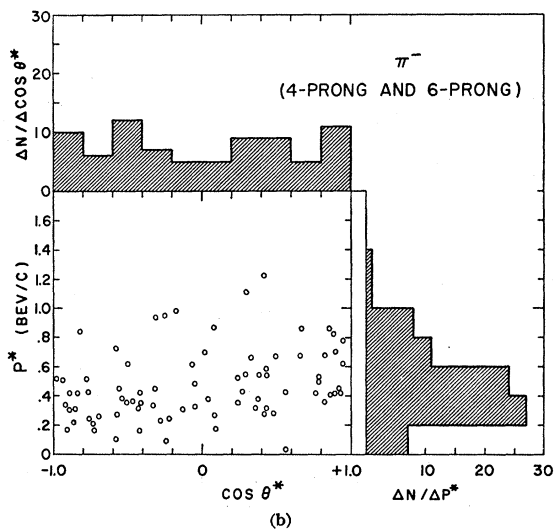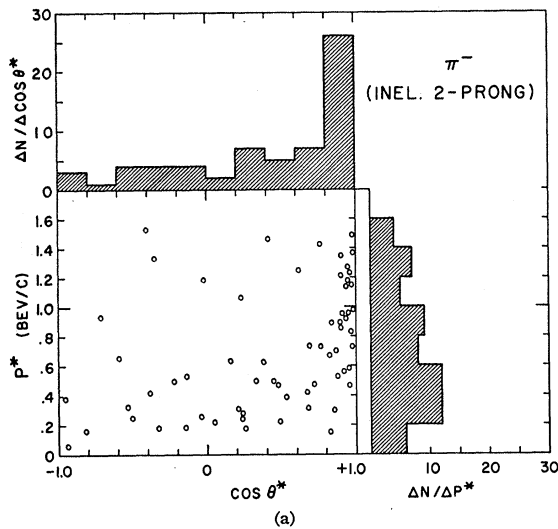
FIG. 8. Center-of-mass scatter diagrams of positive pions from inelastic 2-prong events (upper) and from 4-prong and 6-prong events. Positive particles definitely identified as pions are represented by circles (o) and by the shaded portion of the histograms. Unidentified positive particles (calculated on the basis of a pion mass) are represented by crosses (✕) and by the unshaded portions of the histograms.

We have seen that the distribution of the inelastic events and the average multiplicity of pion production can be fitted by a statistical model with a suitably chosen radius. A more sensitive test of the validity of the statistical model is found in the angular distributions described in the next section.

D. Momentum and Angular Distributions of Inelastic Events

The angular distribution of the elastic events was described in Sec. III-B. We now consider the distributions of momenta and angles of particles emitted in inelastic events. The distributions should, in principle, be plotted separately for each of the various reactions listed in Table I. Not only would extremely poor statistics result from such a detailed division of the events, but also the results would be strongly biased by such a division because events in which the positive particles are emitted backwards in the center-of-mass system are more likely to be uniquely identified. To prevent this bias all the inelastic events were included in the plotted distributions, and the only division was made on the basis of the number of emitted charged particles.

The distributions are presented in the scatter diagrams shown in Figs. 7–11, where momentum is plotted

vs angle in the center-of-mass system. Separate histograms were plotted for high-multiplicity (4 or 6 charged prongs) and low-multiplicity (2-prong) events. Although the 2-prong group contains events involving production of two or more pions, the average multiplicity of the group is somewhat lower than that of the 4-prong events. In about half of all the events the positive particles were not identified as protons or pions. The c.m. momenta and angles were calculated for both possible interpretations and included in the appropriate scatter diagrams. Consequently some of the unidentified tracks in the proton distribution were really pions, and vice versa. When an unidentified positive track is calculated both as a proton and as a pion the resulting c.m. angle of the proton is always greater than that of the pion. The slight forward peak in the angular

distribution of the positive pions, shown in Fig. 8, may therefore be due to protons. However, the backward peaks in the proton distributions, shown in Fig. 7, consist largely of identified protons. Thus, if the unidentified tracks due to pions could be subtracted, a strong backward peak would remain.

In the distributions of negative pions, shown in Fig. 9, there is no ambiguity concerning the masses of the particles. The angular distributions of π^- from 2-prong and 4-prong events are markedly different. An isotropic distribution is found for π^- from 4-prong events, while the negative pions from 2-prong events show a sharp forward peak, which may indicate that low-multiplicity events involve relatively small momentum transfer. Distributions for neutral pions and neutrons are shown in Figs. 10 and 11. They are quite similar to the distributions of the corresponding charged particles but are considered less certain because in most events the possibility that two or more neutral particles were emitted could not be eliminated.

These angular distributions furnish a rather sensitive test of the validity of the statistical theory of multiple pion production. It was shown in the previous section that the number of emitted pions could be fitted by the statistical model with a suitable choice of interaction volume. However, the assumption of statistical equilibrium in the statistical theories requires that the angular distributions of the emitted particles be symmetric about 90° in the c.m. system. The strong asymmetry shown in Figs. 7 and 9 indicates, therefore, that statistical equilibrium is not attained in 5-Bev π^--p collisions.

The momenta of particles from 2-prong events tend to be somewhat higher than the momenta of the corresponding particles from 4- and 6-prong events. This is consistent with the view that the 2-prong events involve relatively low multiplicity and leave more of
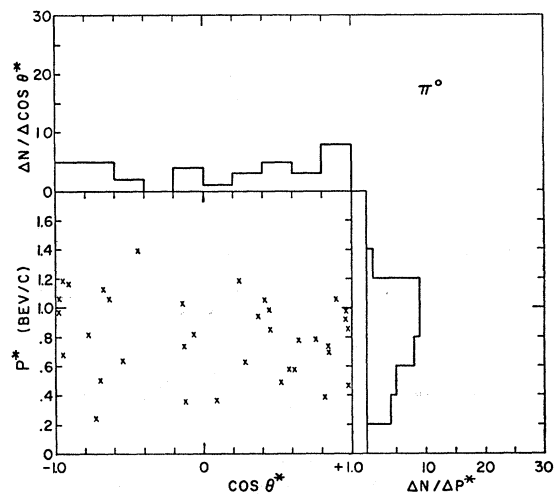

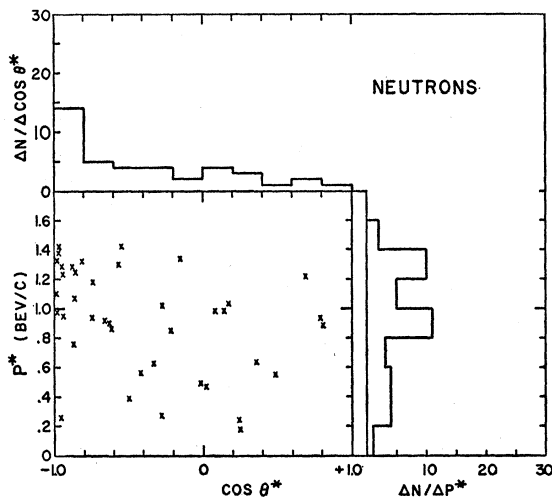FIG. 9. Center-of-mass scatter diagrams of negative pions from inelastic 2-prong events (upper) and from 4-prong and 6-prong events (lower).

FIG. 10. Center-of-mass scatter diagram of neutral pions from all inelastic events consistent with the emission of a single π^0.

the available energy for the charged particles. The momenta and angles of all charged particles are summarized in Fig. 12. The average momentum, in the c.m. system, of all protons is 736 Mev/c, and that of the pions is 537 Mev/c.

E. Angular Correlations and Q Values Between Pairs of Particles

The Brookhaven experiments on π^--p, n-p, and p-p collisions in the 1- to 2-Bev energy range showed rather marked angular correlations between certain pairs of particles emitted from inelastic events.[6,18,25,26] These correlations were consistent with a model in which the production of pions proceeds via an intermediate excited $(T=J=\frac{3}{2})$ nucleon state or is influenced by resonant final-state interactions.[27]

The data of this experiment were examined for correlations that might yield evidence for similar interactions between pairs of emitted particles. Correlation angles and relative kinetic energies (Q values) were calculated for all pairs of particles emitted from inelastic events. The distributions from 2-prong and 4-prong events were quite similar and have been lumped together. Figure 13 shows the distributions of $\cos\theta_{i,j}^*$ for several pairs of particles, where $\theta_{i,j}^*$ is the angle in the c.m. system between the emitted particles i and j. The distributions appear rather isotropic except for a tendency for some nucleons and pions to be emitted in opposite directions. This angular correlation results from the asymmetric angular distributions described in the preceding section. However, a slight correlation
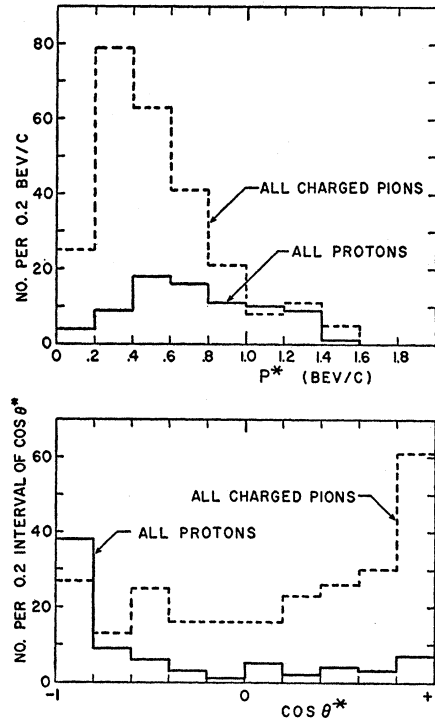
FIG. 12. Center-of-mass momentum and angular distributions of all charged particles from all inelastic events. These histograms are the sums of the histograms shown in Figs. 7, 8, and 9.

would be required by momentum conservation, even in the absence of these asymmetries, because the average c.m. momentum of the protons was found to be 200 Mev/c greater than that of the pions. The distributions involving neutrons are considered much less certain, and may be biased, because in most events the possi-

FIG. 11. Center-of-mass scatter diagram of neutrons from all inelastic events consistent with the emission of a single neutron.

[25] Fowler, Shutt, Thorndike, and Whittemore, Phys. Rev. 95, 1026 (1954).
[26] W. A. Wallenmeyer, Phys. Rev. 105, 1058 (1957).
[27] D. C. Peaslee, Phys. Rev. 94, 1085 (1954); 95, 1580 (1954). J. S. Kovacs, Phys. Rev. 101, 397 (1956).
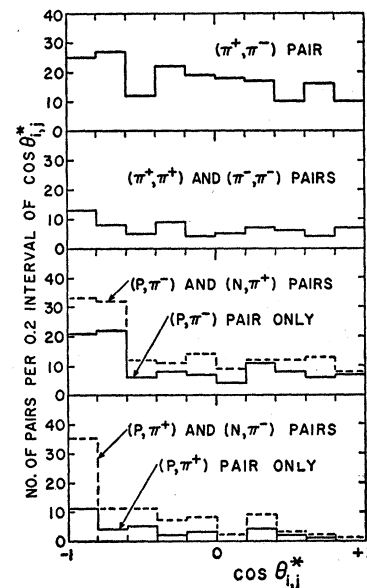
FIG. 13. Distributions of correlation angles, in the c.m. system, between various pairs of particles from all inelastic events.
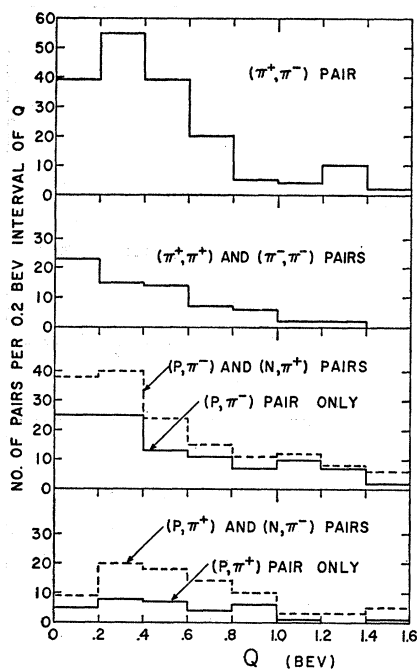
FIG. 14. Distributions of Q values between various pairs of particles from all inelastic events.

bility that two neutral particles were actually emitted could not be ruled out.

The distributions of Q values for these same pairs of particles are shown in Fig. 14. Like the angular correlations, the Q-value distributions show no dramatic effects. If the production of pions proceeds via an excited nuclear isobar with $T=J=\frac{3}{2}$, the Q-value distributions of the (p,π^+) and (n,π^-) pairs should have a rather strong peak at about 160 Mev corresponding to the $\frac{3}{2}$, $\frac{3}{2}$ pion-nucleon scattering resonance. The distributions in Fig. 14 are rather broad and do not show any sharp peaks. The presence of any resonant pion-nucleon or pion-pion interactions might be expected to yield Q distributions of varying shapes. The similarity of the shapes of all the Q distributions indicates, therefore, that this experiment does not furnish evidence for resonant interactions between pairs of emitted particles.

F. Production of Heavy Unstable Particles

Only four of the events involved the production and visible decay of heavy unstable particles. It is quite likely that several of the other inelastic events also involved the production of strange particles that did not decay before leaving the sensitive region of the chamber. If a K meson of about 300 Mev/c were emitted in such an event, it might be recognized by its ionization. In two events tracks appearing to be K^+ mesons were indeed observed, but this identification was not sufficiently certain to justify classifying these events as strange-particle production events.

In addition to these events, the decay of 103 neutral V particles produced by the pion beam in the chamber wall was observed. An analysis of these and 109 additional wall-produced V^0 decays from neutron and proton beam exposures has been published.[12]

Event A, shown in Fig. 15, is interpreted as the associated production of a Λ^0 and a K^+ meson. Tracks 1, 3, and 4 are identified as a K^+, a proton, and a π^- respectively by their momentum and relative ionization (Track 2 is presumably a π^-). If Track 1 were a pion its ionization would be very nearly minimum, and if it were a proton its ionization would be 2.5 times that of Track 4. Consequently its identification as a K^+ seems rather certain. This identification is consistent with the assignment by Gell-Mann and Pais of strangeness $S=-1$ for the Λ^0 and $S=+1$ for the K^+.[28] Lack of energy and momentum balance indicate that one or two neutral pions were produced. The event is therefore interpreted as

$$\pi^-+p\rightarrow K^++\pi^-+\Lambda^0+(\text{one or two }\pi^0).$$
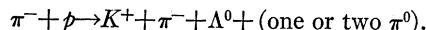
The dihedral angle between the production and decay planes of the Λ^0 was 28°. The visible length of Track 1, the K^+ meson, corresponds to a proper time of flight of
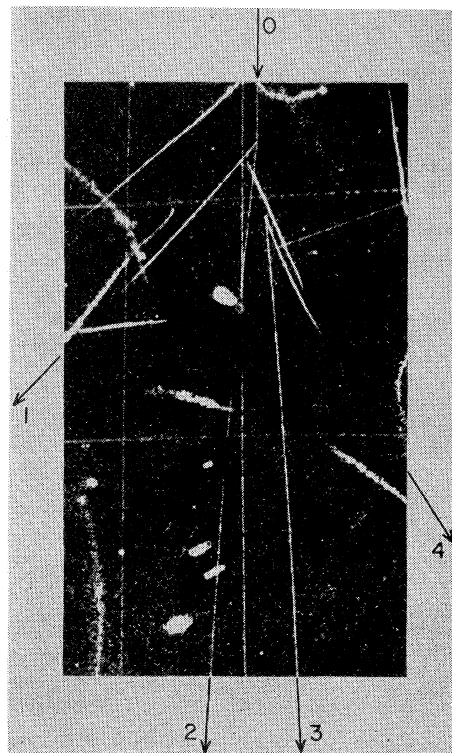

FIG. 15. Event A. The most probable interpretation is that Track 0 is the incident π^-, Track 1 is a K^+ meson, Track 2 is a π^-, and Tracks 3 and 4 are the proton and π^- from a Λ^0 decay.

[28] M. Gell-Mann, Phys. Rev. 92, 833 (1953); M. Gell-Mann and A. Pais, *Proceedings of the 1954 Glasgow Conference on Nuclear and Meson Physics* (Pergamon Press, London, 1955).

only 1/40 of a mean life, so that it is not surprising that no decay was seen.

In Event B, shown in Fig. 16, the decay of both strange particles was observed. The positive prong (Track 2) of the 2-prong event decayed through an angle of 5°, and at the very edge of the cloud chamber a faint V particle was seen (Tracks 3 and 4). Although one can assign only lower limits to the momenta of the two tracks forming the V, the geometry is incompatible with the possibility that this is a Λ^0, but fits a θ^0 of about 970 Mev/c. The positive unstable particle could be either a Σ^+ or a K^+, since the momentum of its decay product is practically unmeasurable. Consequently there are two alternative interpretations for this event:

$$\pi^-+p\rightarrow\pi^-+\Sigma^++\theta^0+(\pi^0),$$
$$\rightarrow\pi^-+K^++\bar{\theta}^0+(n).$$
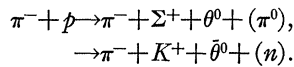
Momentum and energy can be balanced by a π^0 in the first reaction and by a neutron in the second one. The estimated ionization of the positive decaying track and its short lifetime ($\simeq10^{-10}$ sec) favor its interpretation as a Σ^+ rather than a K^+. One may note that the θ in
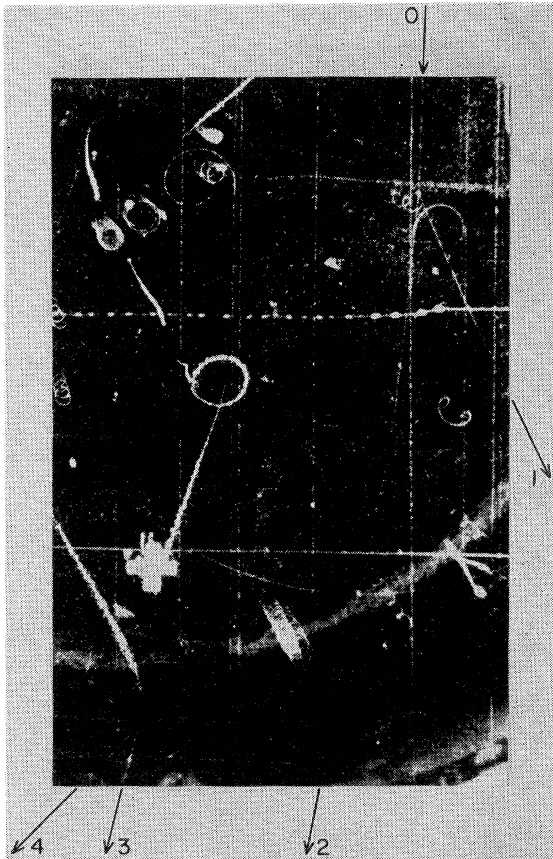

FIG. 16. Event B. Track 0 is the incident π^-, Track 1 is a π^-, Track 2 is a K^+ or a Σ^+ that decays in flight, and Tracks 3 and 4 are pions from a θ^0 decay.
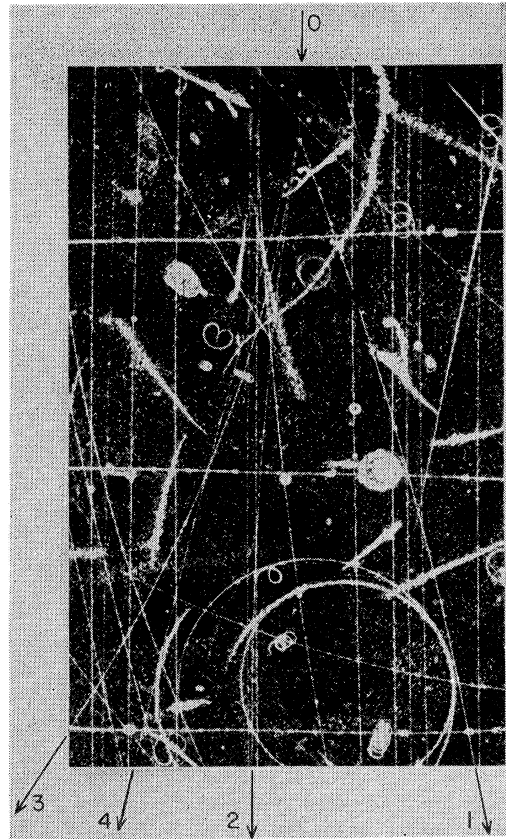

FIG. 17. Event C. Track 0 is the incident π^-, Track 1 is a proton, Track 2 is a π^-, and Tracks 3 and 4 are pions from a θ^0 decay, which occurred about 3 mm from the original π^--p collision.

the second reaction must have strangeness $S=-1$ corresponding to a $\bar{\theta}^0$.

The most interesting event was Event C, shown in Fig. 17, in which a θ^0 was produced together with two charged prongs. All the outgoing tracks are about 20-cm long, and their momenta could be measured to within 5%. Track 1 is identified as a proton or a Σ^+ and Track 3 is a π^+. Interpretation of Track 1 as a Σ^+, however, results in more missing momentum than missing energy for all permissible adjustments of the measurements, and must therefore be ruled out. The θ^0 has a Q value of 222.6 ± 7.7 Mev and a proper lifetime of only 2×10^{-12} sec. The most probable interpretation of the event is

$$\pi^-+p\rightarrow\pi^-+p+\theta^0+(\bar{\theta}^0).$$
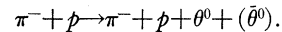
The presence of the $\bar{\theta}^0$ is indicated by a neutral mass of $M_N=502_{-124}^{+91}$ Mev, and is consistent with the associated production of two neutral K particles of opposite strangeness, according to the Scheme of Gell-Mann and Pais. A more detailed description of this event has already been published.[1]

The last event involving strange-particle production and decay was found in an extremely poor picture. A 4-prong star was observed in which one positive out-

860

going particle decayed in flight. The momentum and angle of decay were definitely too large to be consistent with a π-μ decay. The momenta of the other three tracks could not be measured sufficiently well to permit further analysis. However, the presence of four charged outgoing prongs shows that at least one additional pion was emitted together with the heavy unstable particles.

It is interesting to note that in all these collisions pions were produced in addition to the heavy unstable particles. If we combine the four events described above with two similar events produced by 5.3-Bev p-p collisions[3] and nine similar events produced by high-energy n-p collisions,[2] we find that pions were certainly emitted in nine out of the fifteen cases and that all the remaining cases are uncertain and may also have involved pion production. This is not surprising in view of the fact that the energy available in the center-of-mass system ranged up to 2 Bev. It appears, therefore, that strange-particle production without accompanying pion production is quite improbable in elementary-particle collisions at these energies,[29] in contrast to the results at 1.4 Bev,[30] where all the strange-particle production events were interpreted as $\pi^- + p \rightarrow Y + K$.

IV. SUMMARY

The analysis of 137 events resulting in charged outgoing particles shows that inelastic collisions involving production of one or more secondary pions are the predominant processes occurring at 5 Bev (80% of all collisions that result in charged particles). Eight examples of production of four or more secondary pions were observed. The cross section for all processes resulting in charged particles is 21.1 ± 2.3 mb. An estimate of the number of unrecorded zero-prong events yields a total cross section of 22.5 ± 2.4 mb.

The elastic-scattering cross section is 4.7 ± 1.0 mb. Nearly all the elastic events occurred at small angles (less than 9° lab) and were due to diffraction scattering. The diffraction pattern indicates that the region of interaction has a radius of $(0.9 \pm 0.15) \times 10^{-13}$ cm and an opacity of about 0.6.

The relative frequency of events involving production of different numbers of secondary pions could not be uniquely determined because of the many possible reactions and the measurement uncertainties. The observed distribution of the various types of inelastic

events nevertheless yields a rather definite value of 2.3 for the average number of secondary pions per inelastic event. This average multiplicity is greater than that predicted by the Fermi statistical theory of multiple pion production. The predicted average multiplicity can, however, be raised to 2.3 if the interaction radius occurring in the theory is raised to 1.7×10^{-13} cm. The resulting predicted distribution of events of different pion multiplicities is entirely consistent with the observed distribution of events. This average multiplicity and its corresponding interaction radius differ rather strongly from the corresponding values found in anti-proton annihilation in which the available energy is very nearly the same as in this experiment.

Some of the angular distributions of the emitted particles are quite inconsistent with the statistical model's basic assumption of statistical equilibrium. Negative pions from low-multiplicity events are most frequently emitted in the forward direction in the c.m. system and the angular distribution of nucleons from all events has a strong backward peak. The observation that the distributions are not symmetric about 90° in the c.m. system is therefore interpreted as evidence that complete statistical equilibrium was not attained in these collisions.

Angular correlations and Q values were examined for possible evidence of interactions between pairs of emitted particles. The distributions of correlation angles were essentially isotropic. The Q-value distributions were rather broad, and showed no striking effects.

Four events involved the production and visible decay of heavy unstable particles. All four are consistent with the scheme of Gell-Mann and Pais. One of the events is interpreted as the production of a θ^0, $\bar{\theta}^0$ pair. One or more pions were emitted in each of these four events. The combination of these four events with 11 others resulting from high-energy p-p and n-p collisions shows that pion production accompanies the production of strange particles in at least 60% of elementary-particle collisions at Bevatron energies.

[29] W. B. Fowler, *Proceedings of the Sixth Annual Rochester Conference on High-Energy Physics* (Interscience Publishers, Inc., New York, 1956).
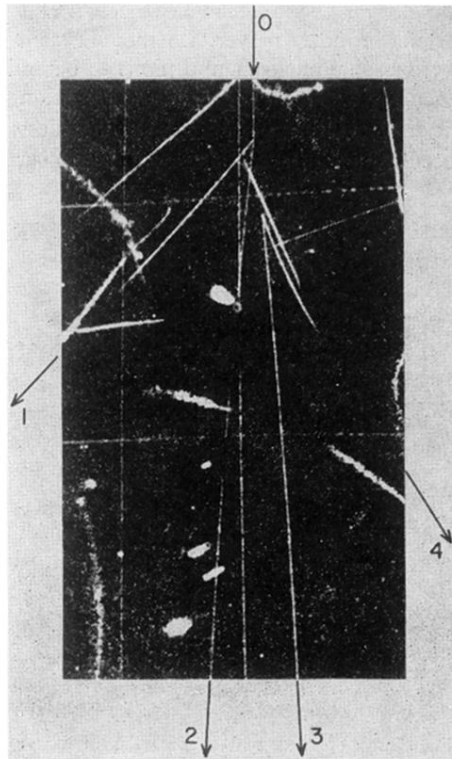[30] Fowler, Shutt, Thorndike, and Whittemore, Phys. Rev. **98**, 121 (1955).

Fig. 15. Event A. The most probable interpretation is that Track 0 is the incident π^-, Track 1 is a K^+ meson, Track 2 is a π^-, and Tracks 3 and 4 are the proton and π^- from a Λ^0 decay.
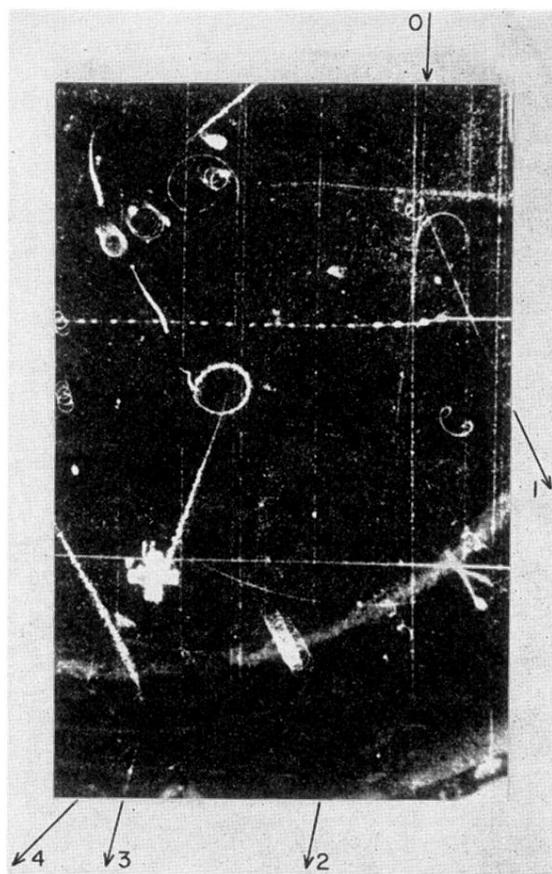
FIG. 16. Event B. Track 0 is the incident π^-, Track 1 is a π^-, Track 2 is a K^+ or a Σ^+ that decays in flight, and Tracks 3 and 4 are pions from a θ^0 decay.
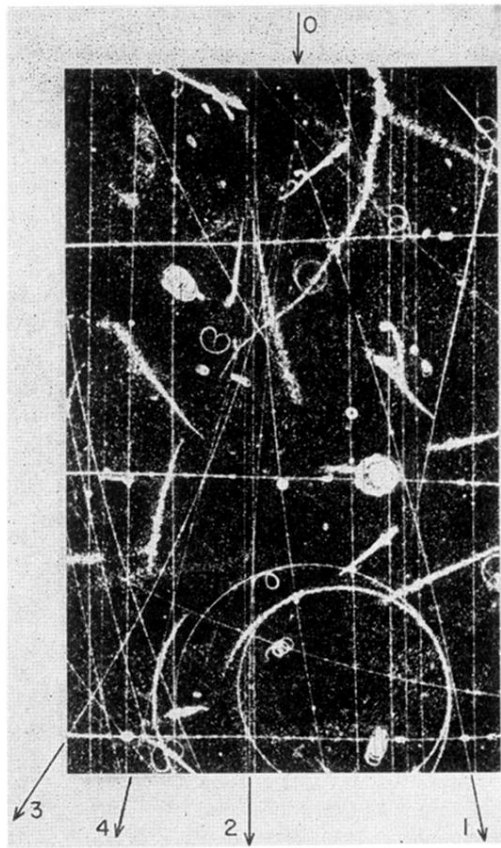
FIG. 17. Event C. Track 0 is the incident π^-, Track 1 is a proton, Track 2 is a π^-, and Tracks 3 and 4 are pions from a θ^0 decay, which occurred about 3 mm from the original π^--p collision.